Force modulating dynamic disorder: A physical model of catch-slip bond transitions in receptor-ligand forced dissociation experiments

Fei Liu[1,*] and Zhong-can Ou-Yang[1,2]
[1]*Center for Advanced Study, Tsinghua University, Beijing, 100084, China*
[2]*Institute of Theoretical Physics, The Chinese Academy of Sciences, P. O. Box 2735 Beijing 100080, China*
(Received 29 May 2006; revised manuscript received 21 August 2006; published 6 November 2006)

Recent experiments found that some adhesive receptor-ligand complexes have counterintuitive catch-slip transition behaviors: the mean lifetimes of these complexes first increase (catch) with initial application of a small external force, and then decrease (slip) when the force is beyond some threshold. In this work we suggest that the forced dissociation of these complexes might be a typical rate process with dynamic disorder. The one-dimensional force modulating Agmon-Hopfield model is used to describe the transitions in the single-bond P-selectin glycoprotein ligand 1-P-selectin forced dissociation experiments, which were respectively performed in the constant force [Marshall *et al.*, Nature (Landon) **423**, 190 (2003)] and the ramping force [Evans *et al.*, Proc. Natl. Acad. Sci. U.S.A **98**, 11281 (2004)] modes. We find that, an external force can not only accelerate the bond dissociation, but also modulate the complex from the lower-energy barrier to the higher one; the catch-slip bond transition can arise from a particular energy barrier shape. The agreement between our calculation and the experimental data is satisfactory.

DOI: 10.1103/PhysRevE.74.051904 PACS number(s): 87.15.Aa, 82.37.Rs, 87.15.By, 82.20.Uv

I. INTRODUCTION

Adhesive receptor-ligand complexes with unique kinetic and mechanical properties play key roles in cell aggregation, adhesion and other life functions in cells. A well-studied example is the receptors in the selectin family, which comprises E-, L-, and P-selectin, interacting and forming "bonds" with their ligands. These bonds are primarily responsible for the tethering and rolling of leukocytes on inflamed endothelium under shear stress [1,2]. Recently, great experimental effort [3–7] has been devoted to studying the intriguing kinetic and mechanical behaviors of the bonds between L- and P-selectin and P-selectin glycoprotein ligand 1 (PSGL-1) at the single-molecule level: the lifetimes of these bonds first increase with initial application of a small force, ("catch" bonds) and subsequently decrease ("slip" bonds) when the force increases beyond some threshold. The biological relevance of this discovery is that the catch-slip transitions of the PSGL-1–L- and P-selectin bonds may provide direct experimental evidence at the single-molecule level to account for the shear threshold effect [8,9], in which the number of rolling leukocytes on the vascular wall first increases and then decreases while monotonically increasing shear stress.

On the theoretical side, Bell [10] first suggested that the forced dissociation rate of adhesive receptor-ligand complexes could be described by

$$k_{\mathrm{off}}(f) = k_{\mathrm{off}}^{0} \exp(f_{\parallel} \xi^{\ddagger} / k_{\mathrm{B}} T), \tag{1}$$

where

$$k_{\mathrm{off}}^{0} = k_{0} \exp(-\Delta G^{\ddagger} / k_{\mathrm{B}} T) \tag{2}$$

is the intrinsic dissociation rate in the absence of force, $\Delta G^{\ddagger}$ is the height of the intrinsic energy barrier, $\xi^{\ddagger}$ is the distance from the bound state to the energy barrier, $f_{\parallel}$ is a projection of the external applied force f onto the dissociation coordinate and is thought to be positive, k_{B} is Boltzmann's constant, and T is absolute temperature. The validity of the expression was supported in various experiments [11,12]. The Bell expression cannot explain catch bonds because force in this model only lowers the height of the energy barrier and shortens the bond lifetimes. In the past two years three chemical kinetic models were developed to quantitatively understand the intriguing catch-slip bond transitions. Evans *et al.* presented a two-pathway and two-bound-state model with assumption of rapid equilibrium between the two states. They suggested that the catch-slip bond transitions take place due to the applied force switching the pathway with faster dissociation rate to the other with a slower one [4]. The next model given by Barsegov and Thirumalai [13] has almost the same kinetic scheme except that the applied force acts on the two dissociation pathways simultaneously. Very recently, a competitive two-pathway and one-bound-state model was proposed by Thomas *et al.* [14]. This model is distinct from the others because there is a catch pathway therein, which was thought to have a negative force projection on the dissociation coordinate [15].

Although these discrete chemical kinetic models explain the catch-slip bond transition and fit the experimental data well, we are still interested in this issue because we recently found that an alternative mechanism, i.e., a stronger positive correlation between the fluctuating intrinsic energy barrier $\Delta G^{\ddagger}$ and the distance $\xi^{\ddagger}$ [16], can also induce the transition. The assumption of our work was that the energy barrier and distance in Eq. (1) are fluctuating with time due to either global conformational changes or local conformational changes at the interfaces. This is plausible because the interface between PSGL-1 and L- or P-selectin is very broad and shallow [17]. We know that chemical reactions with fluctuating energy barrier have usually been called rate processes with dynamic disorder [18]; our model therefore could be

*Email address: liufei@tsinghua.edu.cn

viewed as a natural extension of this concept to the forced dissociation cases. Even so, this model is not satisfactory quantitatively. Our model predicted the mean lifetime of the PSGL–P-selectin bond to be symmetric relative to the transition force f_t, whereas the data [3] were clearly skewed toward a large force. Also, this model did not fit the two experiments performed, respectively, in the constant [3] and ramping force [4] modes with the same set of parameters.

To overcome these shortages, in the present work we suggest a different model to re-explain the catch-slip bond transition. As a continuance of our previous work, we still describe the forced dissociation of the PSGL-1–L- or P-selectin complex as a rate process with dynamic disorder. The additional assumption and key point in this model is that the external force can act on the inner conformational coordinate of the complex simultaneously, while the coordinate is a "hidden" variable in the experiment. Therefore, the force not only lowers the height of the energy barrier as described in Eq. (1) but also modulates the distribution of the coordinate. If the force stabilizes the complex by dragging the system to the states with higher-energy barrier, and this effect is larger than the forced dissociation reaction, the complex presents a catch behavior to the force; otherwise a slip bond is observed. The catch-slip bond transition can be induced at a particular energy barrier with respect to the conformational coordinate. Our calculation agrees with the experimental data well.

The organization of the paper is as follows. In the next section, we describe the physical assumption of the force modulating diffusion-reaction equation and present the essential mathematic derivations. In Sec. III, we study three mean lifetimes for three kinds of energy barrier function with respect to the conformational coordinate: the linear, harmonic, and piecewise functions with two segments. In particular, the last one is used to fit the experimental data. Finally we present the conclusion.

II. THEORY AND METHODS

The physical assumption of our model is very similar to that of a small ligand binding to heme proteins [19]: there is an energy surface for complex dissociation that depends on both the reaction coordinate for the dissociation and the conformational coordinate x, and the latter is perpendicular to the former; for each conformation x there is a different dissociation rate constant obeying the Bell expression; the distribution of x could be modulated by a component of the external force along the x direction; higher temperature or larger diffusivity (low viscosities) allows x variation within the complex to take place, which results in a variation of the energy barrier of the bond with time.

A. The constant force mode

There are two types of experimental setups to measure the forced dissociation of receptor-ligand complexes. We first consider the constant force mode [3,5]. The diffusion equation in the presence of a coordinate-dependent reaction is given by [19]

$$\frac{\partial p(x,t)}{\partial t} = D\frac{\partial^2 p}{\partial x^2} + \frac{D}{k_B T}\frac{\partial}{\partial x}\left(p\frac{\partial V_{f_\perp}}{\partial x}\right) - k_{\text{off}}(x,f_\parallel)p, \tag{3}$$

where $p(x,t)$ is the probability density for finding a value x at time t and the density at initial time is thought to be the thermal equilibrium with the potential $V_{f_\perp}$, D is the diffusion coefficient, $f_\perp$ and $f_\parallel$ are the projections of the external force f on the directions of the reaction and conformational coordinates,

$$f_\perp = f\sin\theta,$$

$$f_\parallel = f\cos\theta \geqslant 0, \tag{4}$$

and θ is the angle between f and the reaction coordinate. Equation (3) assumes that the dissociation process is under the influence of a coordinate-dependent Bell rate $k_{\text{off}}(x,f_\parallel)$ and a force modulating potential

$$V_{f_\perp}(x) = V_i(x) - f_\perp x, \tag{5}$$

where $V_i(x)$ is the intrinsic potential in the absence of force. Instead of studying general potentials, in the present work we focus on the harmonic potential

$$V_i(x) = V_0 + \kappa(x - x_0)^2/2 \tag{6}$$

with a spring constant κ. We divide $V_{f_\perp}(x)$ into two parts, i.e.,

$$\begin{aligned} V_{f_\perp}(x) &= V\left(x - x_0 - \frac{f_\perp}{\kappa}\right) + W(f_\perp) \\ &= \frac{\kappa}{2}\left(x - x_0 - \frac{f_\perp}{\kappa}\right)^2 + V_0 - f_\perp x_0 - \frac{f_\perp^2}{2\kappa}. \end{aligned} \tag{7}$$

Defining a new coordinate variable

$$y = x - x_0 - f_\perp/\kappa, \tag{8}$$

we can reexpress Eq. (3) in the y coordinate as

$$\frac{\partial \rho(y,t)}{\partial t} = D\frac{\partial^2 \rho}{\partial y^2} + \frac{D}{k_B T}\frac{\partial}{\partial y}\left(\rho\frac{\partial V(y)}{\partial y}\right) - k_f(y)\rho \tag{9}$$

where $k_f(y) = k_{\text{off}}(y + x_0 + f_\perp/\kappa, f_\parallel)$. Compared to the original work by Agmon and Hopfield [19], our problem for the constant force case is almost the same except the reaction rate now is controlled by an external force. All results obtained by them can be inherited with minor modifications. Here we present only the essential definitions and calculations.

Substituting

$$\rho(y,t) = N_0 \exp\left(-\frac{V(y)}{2k_B T}\right)\phi(y,t) \tag{10}$$

into Eq. (9), we convert the diffusion-reaction equation into the Schrödinger-like presentation [20]

$$\frac{\partial \phi}{\partial t} = D\frac{\partial^2 \phi}{\partial y^2} - U_f(y)\phi = -\mathcal{H}_f(\phi), \tag{11}$$

where N_0 is the normalization constant of the density function $\rho(y,t)$ at $t=0$, and the "effective" potential

$$U_f(y) = U(y) + k_f(y) = \frac{D}{2k_BT}\left[\frac{1}{2k_BT}\left(\frac{dV}{dy}\right)^2 - \frac{d^2V}{dy^2}\right] + k_f(y). \tag{12}$$

We define $U(y)$ to be independent of the force f in the y coordinate. Equation (11) can be solved by the eigenvalue technique [19]. At the large D of interest here, only the smallest eigenvalue $\lambda_0(f)$ contributes to the eigenvalue expansion. It is impossible to analytically get $\lambda_0(f)$ for $k_f(y)$, which we study below. The perturbation approach [21] has to be applied. If the eigenfunctions and eigenvalues of the "unperturbed" Schrödinger operator

$$\mathcal{H} = -D\frac{\partial^2}{\partial y^2} + U(y) \tag{13}$$

in the absence of $k_f(y)$ are known,

$$\mathcal{H}u_n = -\varepsilon_n u_n, \tag{14}$$

the first eigenfunction $\phi_0(f)$ and eigenvalue $\lambda_0(f)$ of the operator $\mathcal{H}_f$ then are respectively given by

$$\phi_0(f) = u_0 + \sum_{m\neq 0} \frac{\int u_0(y)k_f(y)u_m(y)dy}{\varepsilon_0 - \varepsilon_m} u_m + \cdots \tag{15}$$

and

$$\lambda_0(f) = \lambda_0^{(0)}(f) + \lambda_0^{(1)}(f) + \lambda_0^{(2)}(f) + \cdots = \varepsilon_0 + \int u_0(y)k_f(y)u_0(y)dy + \sum_{m\neq 0} \frac{\left[\int u_0(y)k_f(y)u_m(y)dy\right]^2}{\varepsilon_0 - \varepsilon_m} + \cdots. \tag{16}$$

Considering that the system is in thermal equilibrium at the initial time, the first eigenvalue ε_0 must vanish. On the other hand, because

$$u_0(y) \propto \exp[-V(y)/2k_BT], \tag{17}$$

and the square of $u_0(y)$ is just the equilibrium Boltzmann distribution $p_{eq}(y)$ with the potential $V(y)$, we rewrite the first correction to $\lambda_0(f)$ as

$$\lambda_0^{(1)}(f) = \int p_{eq}(y)k_f(y)dy. \tag{18}$$

Substituting the above formulas into Eq. (10), the probability density function then is approximated by

$$\rho(y,t) \approx N_0 \exp\left(-\frac{V}{2k_BT}\right)\exp[-\lambda_0(f)t]\phi_0(f). \tag{19}$$

The quantity measured in the constant force dissociation experiments is the mean lifetime of a bond, $\langle\tau\rangle$,

$$\langle\tau\rangle = -\int_0^\infty t\frac{dQ}{dt}dt = \int_0^\infty Q(t)dt, \tag{20}$$

where the survival probability $Q(t)$ related to the probability density function is given by

$$Q(t) = \int p(x,t)dx = \int \rho(y,t)dy. \tag{21}$$

B. The dynamic force mode

In addition to the constant force mode, the force may be time dependent, e.g., the linear ramping force in a biomembrane force probe (BFP) experiment [4]. We still use Eq. (3) to describe the bond dissociation processes induced by a dynamic force. In order to distinguish this from the constant force mode, we denote the two components of the time-dependent force as $f_{t_\perp}$ and $f_{t_\parallel}$. We still follow Eq. (8) and rewrite Eq. (3) in the coordinate y as

$$\frac{\partial\rho(y,t)}{\partial t} = D\frac{\partial^2\rho}{\partial y^2} + \frac{D}{k_BT}\frac{\partial}{\partial y}\left[\rho\frac{\partial}{\partial y}V\left(y + \frac{k_BT}{D\kappa^2}\frac{df_{t\perp}}{dt}\right)\right] - k_{f_t}(y)\rho, \tag{22}$$

where $k_{f_t}(y) = k_{off}[y + x_0 + f_{t_\perp}/\kappa, f_{t_\parallel}]$, and we have used the property of the harmonic potential. The reader is reminded that the initial density function $p(x,0)$ now is in thermal equilibrium with the intrinsic potential $V_i(x)$ because no force is added at $t=0$. Compared to Eq. (9), the time-dependent term in the parentheses is a consequence of the time-dependent force. It also means that the minimum of the harmonic potential is moving with a velocity proportional to $d^2f_\perp/dt^2$ in the y- "reference frame." Specially, when the dynamic force is ramping, i.e., $f(t) = f_0 + rt$, where r is a constant loading rate, and the zero or nonzero of f_0, respectively, corresponds to the steady or jump force mode [4], this velocity vanishes. It is impossible to analytically solve this diffusion-reaction equation with a time-dependent potential and reaction term; some reasonable approximations would be essential. We assume that the force loading process is very slow compared to the conformational diffusion along the y direction, i.e., $rk_BT/D\kappa^2 \ll 1$. The above equation then reduces to Eq. (9) except that the force in the reaction term is no longer a constant. We also convert the approximated diffusion-reaction equation to a Schrödinger-like representation, and get the same Eqs. (11) and (12) except that the forces therein are replaced by function f_t. Because in this case the effective potential has a time variable, we make use of an adiabatic approximation analogous to what is done in quantum mechanics. The correction of this assumption would be verified by the agreement between theoretical calculation and experimental data. We immediately have

$$\phi(y,t) \approx \exp\left(-\int_0^t [\lambda_0(f_{t'}) + B(f_{t'})]dt'\right)\phi_0(f_t), \tag{23}$$

where the "Berry phase" [21]

$$B(f_t) = \int \phi_0(f_t)\frac{\partial}{\partial t}\phi_0(f_t)dy, \tag{24}$$

and $\phi_0(f_t)$ is the first eigenfunction of the time-dependent Schrödinger operator

$$\mathcal{H}_{f_t} = \mathcal{H} + k_{f_t}(y). \tag{25}$$

Because the eigenvalues and eigenfunctions of the above operator cannot be solved analytically for general k_{f_t}, we apply the perturbation approach again. We obtain $\phi_0(f_t)$ and $\lambda_0(f_t)$ by replacing k_f in Eqs. (15) and (16) with k_{f_t}. The Berry phase then is approximated by

$$B(f_t) \approx \sum_{m\neq 0}\left(\frac{1}{\varepsilon_m}\right)^2 \int u_0(y)k_{f_t}(y)u_m(y)dy \times \int u_0(y)\frac{dk_{f_t}}{dt}u_m(y)dy. \tag{26}$$

Finally, the survival probability for the dynamic force is

$$Q(t) \approx \exp\left(-\int_0^t [\lambda_0(f_{t'}) + B(f_{t'})]dt'\right). \tag{27}$$

Unlike the constant force mode, the data of the dynamic force experiments are typically presented in terms of a force histogram, which corresponds to the probability density of the dissociation forces,

$$P(f) = -\frac{dQ}{dt}\Big/\frac{df}{dt}. \tag{28}$$

For the ramping force case we have

$$P(f,f_0) \approx \frac{1}{r}[\lambda_0(f) + B(f)]\exp\left(-\frac{1}{r}\int_{f_0}^{f}[\lambda_0(f') + B(f')]df'\right). \tag{29}$$

III. RESULTS

Given a bounded diffusion in the harmonic potential Eq. (6), $\mathcal{H}$ reduces to a harmonic oscillator operator with

$$U(y) = \frac{D\kappa}{2k_BT}\left(\frac{\kappa y^2}{2k_BT} - 1\right). \tag{30}$$

Its eigenvalues and eigenfunctions are

$$\varepsilon_n = nD\kappa/k_BT \tag{31}$$

and

$$u_n(z) = 2^{-n/2}\pi^{-1/4}(n!)^{-1/2}e^{-z^2/2}H_n(z), \tag{32}$$

respectively, where $z=(\kappa/2k_BT)^{1/2}y$ and $H_n(z)$ is the Hermite polynormial [21]. As a minimal model, we assume that the Bell expression depends on the conformational coordinate through the intrinsic height of the energy barrier $\Delta G^{\ddagger}$ in Eq. (2) while holding the distance $\xi^{\ddagger}$ fixed. According to the shape of the barrier with respect to the conformational coordinate, we analyze three cases: the linear, harmonic, and piecewise functions.

A. Bell-like forced dissociations

The simplest function of the energy barrier might be linear [19],

$$\Delta G^{\ddagger}(x) = \Delta G_0^{\ddagger} + k_g(x - x_0). \tag{33}$$

According to Eqs. (16) and (26), we easily get

$$\lambda_0^{(1)}(f) = k_0\exp\left(-\beta\Delta G_0^{\ddagger} + \frac{\beta k_g^2}{2\kappa}\right)\exp\left[\beta\left(\xi^{\ddagger}f_{\parallel} - \frac{k_g}{\kappa}f_{\perp}\right)\right],$$

$$\lambda_0^{(2)}(f) = \frac{-k_0^2}{\beta D\kappa}\exp\left(-2\beta\Delta G_0^{\ddagger} + \frac{\beta k_g^2}{\kappa}\right) \times \exp\left[2\beta\left(\xi^{\ddagger}f_{\parallel} - \frac{k_g}{\kappa}f_{\perp}\right)\right]\sum_{n=1}^{\infty}\frac{1}{nn!}\left(\frac{\beta k_g^2}{\kappa}\right)^n, \tag{34}$$

and

$$B(f_t) = \frac{d}{dt}\left(\xi^{\ddagger}f_{t\parallel} - \frac{k_g}{\kappa}f_{t\perp}\right)\frac{k_0^2}{\beta D^2\kappa^2}\exp\left(-2\beta\Delta G_0^{\ddagger} + \frac{\beta k_g^2}{\kappa}\right) \times \exp\left[2\beta\left(\xi^{\ddagger}f_{t\parallel} - \frac{k_g}{\kappa}f_{t\perp}\right)\right]\sum_{n=1}^{\infty}\frac{1}{n^2n!}\left(\frac{\beta k_g^2}{\kappa}\right)^n, \tag{35}$$

where $\beta=1/k_BT$. For large D or κ (or very small T), the second correction and the Berry phase tend to zero. Under these limitations the first eigenvalue of Eq. (3) is approximated to be

$$\lambda_0(f) \approx k_0\exp\left(-\beta\Delta G_0^{\ddagger} + \frac{\beta k_g^2}{2\kappa}\right)\exp(\beta d^{\ddagger}f). \tag{36}$$

Here we define a new distance

$$d^{\ddagger} = \xi^{\ddagger}\cos\theta - \zeta\sin\theta, \tag{37}$$

where $\zeta=k_g/\kappa$. We see that the presence of the complex conformational coordinate can modify the original Bell model: (i) for $d^{\ddagger}>0$, Eq. (36) is indistinguishable from the original Bell model; (ii) for $d^{\ddagger}=0$, the force does not affect dissociations of the bonds, which were termed "ideal" bonds by Dembo [15]; (iii) for $d^{\ddagger}<0$, the force slows down dissociation of the bonds, or a catch bond is observed. This reflects a competition between the two contrasting effects of the same force for $k_g>0$: increase of the force not only destabilizes the molecular complex by lowering the energy barriers (slip), but also stabilizes the bond by dragging the system to the states with higher-energy barrier (catch) simultaneously; if the effect of the latter is larger than that of the former, a catch bond results.

B. Dembo-like forced dissociations

A relatively complicated function of the energy barrier is a harmonic with a spring constant η_g,

$$\Delta G^{\ddagger}(x) = \Delta G_1^{\ddagger} + \eta_g (x - x_1)^2/2, \tag{38}$$

where $\Delta G_1^{\ddagger}$ is the barrier height at position x_1. Because, for any form of the barrier height, the dependence of $\lambda_0^{(2)}(f)$ and $B(f_t)$ on D is the same according Eq. (31), we only consider the large-D limitation in the following part. We have

$$\lambda_0(f) \approx k_0 \left(\frac{\kappa}{\kappa + \eta_g}\right)^{1/2} \exp(-\beta \Delta G_1^{\ddagger} + \beta \xi^{\ddagger} f_{\parallel}) \times \exp\left(-\frac{\beta \eta_g [f_{\perp} - \kappa(x_1 - x_0)]^2}{2\kappa(\kappa + \eta_g)}\right). \tag{39}$$

We also define the distance

$$D^{\ddagger} = \xi^{\ddagger} \cos\theta + 2\eta_g (x_1 - x_0) \sin\theta / (\kappa + \eta_g). \tag{40}$$

Given $D^{\ddagger} > 0$, there is a transition from slip to catch when the force increases over a threshold

$$D^{\ddagger} \kappa (\kappa + \eta_g)/2\eta_g \sin^2\theta; \tag{41}$$

otherwise only a catch bond results. We note that the latter is very similar to the Hookean spring model proposed by Dembo [15] even though their physical origins are completely different: both of them are exponentially dependent on the force square.

C. Comparison with the experiments

1. The constant force mode

In the constant force dissociation experiment of the PSGL-1–P-selectin complex, the dissociation rate first decreased and then increased when force increased beyond a threshold [3]. We can now understand this transition according to the discussion about the Bell-like dissociation rate: the dissociation effect of $f_{\parallel}$ regains its dominance when the force is beyond the threshold. Although there are lots of barrier shapes that can result in a catch-slip transition, the simplest case may be a piecewise function with two segments

$$\Delta G^{\ddagger}(x) = \begin{cases} \Delta G_c^{\ddagger}(x) = \Delta G_b^{\ddagger} + k_c (x - x_b), & x \leqslant x_b, \\ \Delta G_s^{\ddagger}(x) = \Delta G_b^{\ddagger} + k_s (x - x_b), & x > x_b, \end{cases} \tag{42}$$

where we require that the distances defined by Eq. (37) with k_c and k_s are, respectively, negative and positive. For convenience, the absolute values of the distances are denoted by $d_c^{\ddagger}$ and $d_s^{\ddagger}$. Define two "intrinsic" dissociation constants

$$k_0^c = k_0 \exp[-\beta \Delta G_c^{\ddagger}(x_0)],$$

$$k_0^s = k_0 \exp[-\beta \Delta G_s^{\ddagger}(x_0)]. \tag{43}$$

Figure 1 shows the characteristics of the function. We then have

$$\lambda_0(f) \approx \frac{k_0^c}{2} \exp\left(\frac{\beta k_c^2}{2\kappa}\right) \exp(-\beta d_c^{\ddagger} f) \operatorname{erfc}\left[-\left(\Delta + \frac{k_c}{\kappa}\right)\sqrt{\frac{\beta\kappa}{2}} + f\sqrt{\frac{\beta}{2\kappa}} \sin\theta\right] + \frac{k_0^s}{2} \exp\left(\frac{\beta k_s^2}{2\kappa}\right) \exp(\beta d_s^{\ddagger} f) \times \operatorname{erfc}\left[\left(\Delta + \frac{k_s}{\kappa}\right)\sqrt{\frac{\beta\kappa}{2}} - f\sqrt{\frac{\beta}{2\kappa}} \sin\theta\right], \tag{44}$$

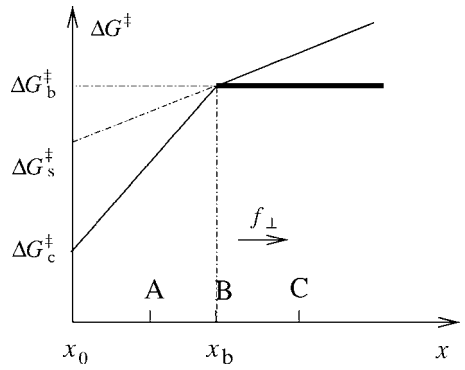

FIG. 1. Schematic diagram of the height function of the energy barrier with respect to the coordinate x (the solid lines). $\Delta G_s^{\ddagger}$ and $\Delta G_c^{\ddagger}$ are the values of the linear functions in Eq. (42) at position x_0, while $\Delta G_b^{\ddagger}$ is the intersection of the functions at x_b.

where $\Delta = x_b - x_0$, and the complementary error function is

$$\operatorname{erfc}(x) = \frac{2}{\sqrt{\pi}} \int_x^{\infty} e^{-x^2} dx. \tag{45}$$

Before fixing the parameters in Eq. (44), we first analyze the main properties of $\lambda_0(f)$ given $\Delta \gg 0$: (i) in the absence of force, due to $\operatorname{erfc}(-\infty) = 2$ and $\operatorname{erfc}(+\infty) = 0$, we have

$$\lambda_0 = k_0^c \exp(\beta k_c^2/2\kappa), \tag{46}$$

which is the same as that obtained by Agmon and Hopfield [19]; (ii) if the force is nonzero and smaller,

$$\lambda_0 \approx k_0^c \exp(\beta k_c^2/2\kappa) \exp(-\beta d_c^{\ddagger} f), \tag{47}$$

which means that the bond is a catch bond; and finally (iii), when the force is sufficiently large, Eq. (44) reduces to

$$\lambda_0 \approx k_0^s \exp(\beta k_s^2/2\kappa) \exp(\beta d_s^{\ddagger} f), \tag{48}$$

which is the ordinary slip bond.

There are in total eight independent parameters in Eq. (44): θ, κ, k_c, k_s, Δ, $\xi^{\ddagger}$, k_0, and $\Delta G_c^{\ddagger}(x_0)$. Through fitting the existing data [3], we can only determine some combinations of them, e.g., k_0^c, $d_s^{\ddagger}$, etc. But if we artificially assume the slope $k_s = 0$ (the bold solid line in Fig. 1) and $\theta = \pi/6$, we immediately have $\kappa \approx 0.21$ pN nm^{-1}, $k_c \approx 0.60$ pN, $\Delta \approx 33$ nm, $\xi^{\ddagger} \approx 0.25$ nm, $k_0^c \approx 23$ s^{-1}, and $k_0^s \approx 1.7$ s^{-1}. Here the particular angle and k_s are actually of no particular significance and we use them only as a reference. We note that Δ is larger than the size of the native complex (~ 10 nm). A possible explanation is that a large sliding or conformational extension occurs along the interface of PSGL-1 and P-selectin before the complex is completely dissociated. Because Δ exists only in the piecewise function case, and its value depends on the choice of θ and k_s, overinterpretation of its meaning is not suitable. Substituting these values into Eq. (44), we calculate the mean lifetime of the PSGL-1–P-selectin complex at different constant forces in Fig. 2; the agreement between theory and the experimental data is good.

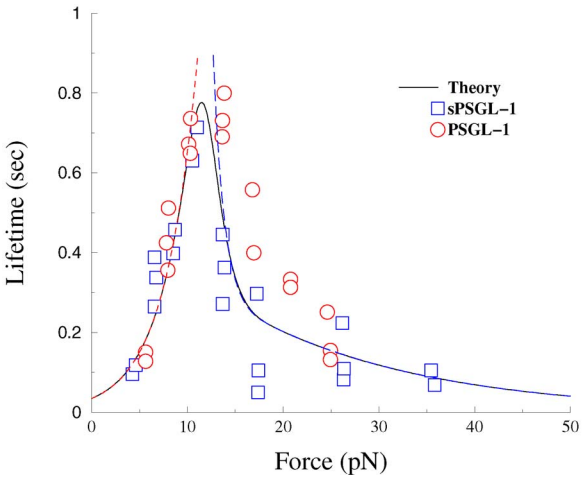

FIG. 2. (Color online) The mean lifetime as a function of force for the bonds of dimeric P-selectin with monomeric sPSGL-1 (square symbols) [3] and the rescaled dimeric PSGL-1 (circle symbols) from Ref. [14]. The solid line is the theoretical fitting. The two dash curves are respectively calculated by the two addition terms in Eq. (44) with the same parameters. Our curve decays faster than that fitted by the two-pathway and one-bound-state model [14] after a transition occurs.

2. The ramping force mode

More challenging experiments for the model are the force steady and jump ramp modes [4]. Under the large-D limitation, Eq. (29) reduces to

$$P(f,f_0) \approx \frac{\lambda_0(f)}{r} \exp\left(-\frac{1}{r}\int_{f_0}^{f} \lambda_0(f')df'\right). \tag{49}$$

We see that the mean lifetime can be extracted from the above equation by setting $f=f_0$, i.e., $\langle\tau\rangle=1/rP(f_0,f_0)$. We first study the general properties of the above equation. The experimental data [4] showed that the force histograms reach the maximum and minimum at two distinct forces, which are named $f_{\min}$ and $f_{\max}$, respectively. This observation is understood by setting the derivative of the density function $P(f,f_0)$ with respect to f equal to zero, i.e.,

$$r\frac{d\lambda_0}{df}(f) = \lambda_0^2(f). \tag{50}$$

Because the left side of the equation is negative for a catch bond, $f_{\min}$ and $f_{\max}$ must be larger than the transition force f_t observed in the constant force mode. On the other hand, Eq. (50) has no solutions when the loading rate is smaller than a critical rate r_c, which is obtained by simultaneously solving Eq. (50) and its first derivative. Applying the parameters obtained from constant force data, we estimate $r_c \approx 6$ pN/s, and $f_{\max}=f_{\min}\approx 13$ pN. Because the density function is a monotonic and decreasing function for $r \leqslant r_c$, the most probable force of bond dissociation is zero. Another quantity of interest is the loading rate dependence of the forces of the maximum and minimum. The latter is an important index in dynamic force spectroscopy theory [22]. When the loading rate is sufficiently large, the approximation of Eq. (47) implies

$$f_{\max} \approx \frac{1}{\beta d_s^{\ddagger}} \ln \frac{\beta r d_s^{\ddagger}}{k_0^s \exp(\beta k_s^2/2\kappa)} \propto \ln r. \tag{51}$$

The experimental measurement supports this conclusion; see Fig. 3A in Ref. [4]. For $f_{\min}$, because it is very close to f_t at the larger loading rate, we employ the Taylor expansion approach and have

$$\lambda_0(f) = \lambda_0(f_t) + \frac{1}{2}\frac{d^2\lambda_0}{df^2}(f_t)(\delta f)^2 + o[(\delta f)^3], \tag{52}$$

where $\delta f=f-f_t$. Substituting it into Eq. (50), we obtain

$$f_{\min} \approx f_t + \lambda_0^2(f_t) \Big/ r\frac{d^2\lambda_0}{df^2}(f_t) \propto r^{-1}, \tag{53}$$

or $f_{\min} \simeq f_t$ at the large loading rate. It also explains why the forces of the minima in the experiment are always around a certain value and seem to be independent of the loading rate (see Figs. 2 and 4 in Ref. [4]). We must emphasize that this prediction is intrinsically characteristic of a catch-slip bond.

When we quantitatively compare the prediction with the real experimental observation, we find that f_t measured by Marshall *et al.* [3] is apparently different from $f_{\min}$ measured by Evans *et al.* [4]; the latter is almost twice as large as the former. Hence it is not unexpected that Eq. (49) based on the parameters from the constant force data cannot fit the dynamic force data. A similar problem was met by Pereverzev *et al.* [14]. They simply contributed it to the different equipment and biological constructs. They used another set of parameters to fit the dynamic force data. The reader is reminded that the two experiments were performed on the same single-bond sPSGL-1–P-selectin complex by the same experimental group. Here we will use the same parameters for the two experiments. But we additionally assume that the BFP experiment performed by Evans *et al.* is for a dimeric-bond sPSGL-1–P-selectin complex: the two independent bonds share the same force and fail randomly. Our consideration is as follows. First, fitting data is not the single aim of a model; complete agreement with the data cannot justify a model. Then we demonstrate that for the forced dissociation of single bond, f_t should be almost the same as $f_{\min}$, while the data showed $f_{\min} \approx 2f_t$. This discrepancy between theory and experiment is easily reconciled if the dimeric-bond assumption was accepted. Finally our calculation fit the dynamic force data well under this assumption; see Fig. 3, where the probability density of the dissociation force for the dimeric-bond PSGL-1–P-selectin complex is related to the single bond by

$$P_d(f,f_0) = P(f/2,f_0/2)^2. \tag{54}$$

Of course, a further experimental test is needed.

IV. DISCUSSION AND CONCLUSIONS

In this work, we present a dynamic model for the catch-slip bond transitions observed in PSGL-1–P-selectin forced dissociation experiments. A possible physical mechanism of the catch bond is suggested here: the applied external force, although it accelerates the dissociation by lowering the

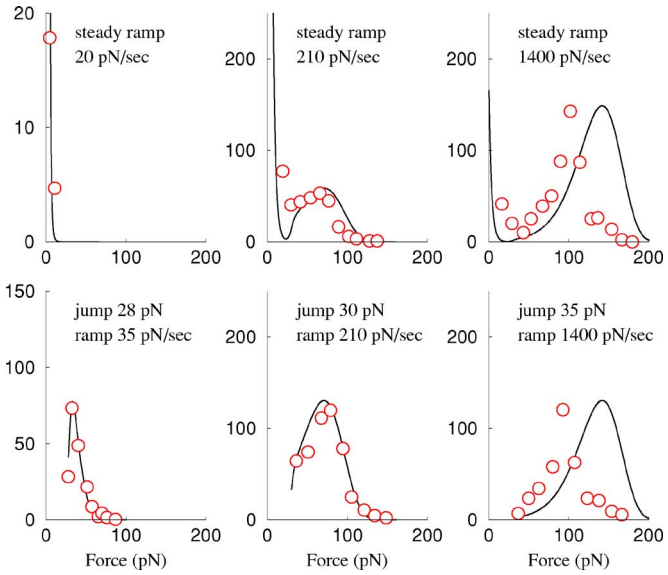

FIG. 3. (Color online) The probability density of the dissociation forces $P_d(f,f_0)$ under the different loading rates predicted by our theory (solid curves) for the PSGL-1–P-selectin complex. The symbols are from the force steady and jump ramp experimental data [4]. We see that the tendencies of our density functions for the first two panels of the second array are closer to the data than that predicted by the two-pathway models [4,14]. The apparent deviations between the theory and the data in the last column may be from the failure of the assumption of the two independent bonds at higher loading rates or the adiabatic approximation.

height of the energy barrier, also stabilizes the complex by dragging the molecule to the state with a higher barrier height; if the effect of the latter is greater than the former, a catch behavior is observed; otherwise a slip bond appears. A piecewise energy barrier is used to quantitatively describe the transitions in the constant and ramping force modes. It is not difficult to "design" a specific complex structure to realize this particular energy surface. Figure 4 shows such a possible example. The inner conformational coordinate x now is a degree of freedom along the interface of the complex. If we simply assume that the energy barrier is proportional to the number of interaction sites between the selectin and PSGL-1, and this number is also proportional to the overlap area of the two molecules, the barrier then has a shape (the bold solid line) depicted in Fig. 1. For instance, the B configuration in the figure corresponds to the bend position of the energy barrier because the interaction is now saturated. Interestingly, the parameter θ in this case has very simple structural interpretation: it is the angle between the interface and the vertical. We believe this picture has some rationalities. We mentioned that the interface of the complex is broad and shallow. Sliding between the two molecules should be very possible under the force $f_\perp$. Moreover, x-ray crystallography structure [17] shows that there is an angle between the epithelial growth factor and lectin (which is responsible for molecular contact) domains in P-or L-selectin, which may result in tilting of the interface toward the force direction and form the angle θ.

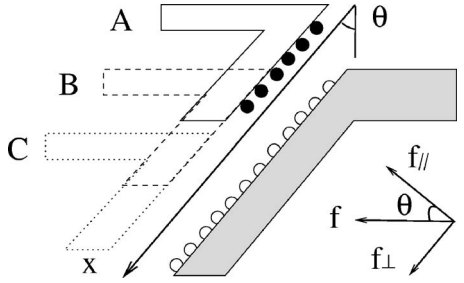

FIG. 4. Schematic of a possible example having a piecewise energy barrier with respect to conformational coordinate x [Eq. (42)]. The force f acting on the PSGL-1 (open regime) is to the left. The interface between selectin (shaded regime) and PSGL-1 makes an angle θ to the vertical. The force then can be broken into two components, $f_\perp$ and $f_\parallel$, which are, respectively, parallel and perpendicular to the interface. Circles (filled and open) represent the interaction sites of the two molecules. The three configurations (A, B, and C) of the selectin correspond to the three coordinates in Fig. 1.

Our force modulating dynamic disorder model has some connections with previous discrete chemical kinetic models [4,13], where force alters the distribution of the two pathways with different dissociation rates. It could be seen by writing Eq. (3) in a finite-difference form [19]. For convenience, we let the force component $f_\parallel=0$. Defining $\Delta x=x_{i+1}-x_i$, $\bar{D}=D\Delta x^2$, $p_i=p(x_i,t)\Delta x$, we have the master equation

$$\frac{\partial p_i}{\partial t} = p_{i-1}k(i|i-1) + p_{i+1}k(i|i+1) - p_i[k(i-1|i) + k(i+1|i)] - k_i p_i \tag{55}$$

where

$$k(i|j) \cong \bar{D}\exp\left(-\frac{V_{f_\perp}(x_i) - V_{f_\perp}(x_j)}{2k_BT}\right). \tag{56}$$

In particular, for only two states, one has the chemical kinetic equation

$$\frac{dp_1}{dt} = p_2k(1|2) - p_1k(2|1) - k_1p_1,$$

$$\frac{dp_2}{dt} = p_1k(2|1) - p_2k(1|2) - k_2p_2. \tag{57}$$

Assuming that the two states are in equilibrium, we easily obtain

$$\frac{dQ}{dt} = -\frac{k_1R + k_2\exp(\beta f\Delta x)}{R + \exp(\beta f\Delta x)}Q \tag{58}$$

where the survival probability $Q=p_1+p_2$, and

$$R = \exp\left(\frac{V_i(x_2) - V_i(x_1)}{k_BT}\right). \tag{59}$$

This is just the model proposed by Evans *et al.* [4]. If $f_\parallel$ does not vanish and $\xi^\ddagger$ is also a function of the conformational coordinate, we should also recover the model proposed by Barsegov and Thirumalai [13]. This discussion also reminds us that the component $f_\perp$ is not indispensable in explaining the catch-slip transitions, which can be seen if we assume

that the energy barrier as a function of coordinate x first increases and then decreases after reaching a maximum. In a quantitative way, we make $\theta=\pi/2$; then the other parameters are $\kappa\approx 0.84$ pN nm^{-1}, $k_c\approx 1$ pN, $k_s\approx -0.22$ pN, $\Delta\approx 16.5$ nm, and k_0^c and k_0^s are the same as those in the $\theta=\pi/3$ case. Because $f_\parallel=0$, the distance $\xi^\ddagger$ is not present. Such an energy surface will occur if the maximum overlap area of the selectin and PSGL-1 is almost the same as their respective contact surfaces.

One may then ask what insight or understanding is obtained by our theory based on the continuum diffusion-reaction description with eight parameters. After all, the simpler discrete two-pathway models with four [14] and five parameters [4] explained the data well. The continuum diffusion-reaction description should be more attractive in the following aspects. First of all, the two-pathway and two-bound-state models [4,13] assume the states are separated by an energy barrier. This assumption seems to be less appropriate than the diffusion scheme for describing conformational dynamics in real proteins [23]. The derivation of Eq. (55) suggests that the discrete scheme might be a mathematical approximation of the continuum case. The "smooth" energy landscape can also lead to the catch-slip bond transitions. Then there are two new physical parameters, the angle θ and diffusion coefficient D in the current model. Although fitting the existing data does not benefit from the two parameters, they might be important to explain other phenomena in which force is involved. For instance, the angle θ may be relevant to the orientational dependence of the adhesion of selectins and their ligands under shear stress [1], which can be seen from Eq. (37): the bond with catch characteristics ($k_g>0$) will alter to the slip case by adjusting the angle to be smaller than

$$\theta_0=\arctan(\xi^\ddagger/\zeta). \tag{60}$$

Because there is structural evidence supporting the existence of the angle, this explanation may be reasonable. The coefficient D, because we assumed that the conformational fluctuation is always fast at any given force, it does not matter in fitting the single-molecule data. But the effect of the diffusion coefficient would appear if the forced dissociation experiment was done at lower temperatures or higher solvent viscosities. An extreme situation is that the viscosity (temperature) is so high (low) that D almost vanishes. The probability density $p(x,t)$ of Eq. (3) then has an analytical solution given by

$$p(x,t)\approx p(x,0)\exp[-tk_{\mathrm{off}}(x,f_\parallel)], \tag{61}$$

where $p(x,0)$ is any initial distribution independent of force. This is a typical example of rate processes with *static disorder* [18]. In addition, the survival probability of the bond converts into a multiple-exponential decay for a single force from the single-exponential decay at the large-D limit (the existing data support the large-D approximation; see Figs. 3(d) and 3(e) in Ref. [3]), the mean lifetime is

$$\langle\tau\rangle\approx\int p(x,0)k_{\mathrm{off}}^{-1}(x,f_\parallel), \tag{62}$$

which means that the catch-slip bond alters into a slip bond only. Finally, we pointed out at the beginning that the counterintuitive catch-slip bond transition is one example of a rate process with dynamic disorder. Because this concept has been deeply studied in theory and experiment during the past two decades, the extensive experience and knowledge would be useful for further experimental and theoretical study of catch-slip bonds.

Although our model has some differences from previous work, we cannot definitely distinguish which theory or model is the most reasonable and closest to real situations with the existing experimental data. Moreover, except for the coarse-grained physical picture our theory does not reveal detailed structural information about the catch behavior of the ligand-receptor complexes, whereas biologists would be interested in it. Further single-molecule experiments including micromanipulation experiments and fluorescence spectroscopy, more crystal structure data, and detailed molecular dynamics simulations from the atomic interactions are essential to elucidate the real molecular mechanism of the catch bonds.

ACKNOWLEDGMENTS

One of the authors (F.L.) would like to thank Professor Mian Long and Dr. Fei Ye for their helpful discussion about the work. F.L. was supported by the National Natural Science Foundation of China (NSFC).

[1] R. P. McEver, Curr. Opin. Cell Biol. **14**, 581 (2002).
[2] K. Koonstantopoulos, S. Kurkreti, and L. V. McIntire, Adv. Drug Delivery Rev. **33**, 141 (1998).
[3] B. T. Marshall *et al.*, Nature (London) **423**, 190 (2003).
[4] E. Evans, A. Leung, V. Heinrich, and C. Zhu, Proc. Natl. Acad. Sci. U.S.A. **101**, 11281 (2004).
[5] K. K. Sarangapani *et al.*, J. Biol. Chem. **279**, 2291 (2003).
[6] T. Yago *et al.*, J. Cell Biol. **166**, 913 (2004).
[7] B. T. Marshall *et al.*, Biophys. J. **88**, 1458 (2005).
[8] E. B. Finger *et al.*, Nature (London) **279**, 266 (1996).
[9] M. B. Lawrence, G. S. Kansas, E. J. Kunkel, and K. Ley, J. Cell Biol. **136**, 717 (1997).
[10] G. I. Bell, Science **136**, 618 (1978).
[11] R. Alon, D. A. Hammer, and T. A. Springer, Nature (London) **374**, 539 (1995).
[12] S. Chen and T. A. Springer, Proc. Natl. Acad. Sci. U.S.A. **98**, 950 (2001).
[13] V. Barsegov and D. Thirumalai, Proc. Natl. Acad. Sci. U.S.A. **102**, 1835 (2005).
[14] Y. V. Pereverzev *et al.*, Biophys. J. **89**, 1446 (2005).
[15] M. Dembo, D. C. Tourney, K. Saxman, and D. Hammer, Proc. R. Soc. London, Ser. B **234**, 55 (1988).

[16] F. Liu, Z.-C. Ou-Yang, and M. Iwamoto, Phys. Rev. E **73**, 010901(R) (2006).
[17] W. S. Somers, J. Tang, G. D. Shaw, and R. T. Camphausen, Cell **103**, 467 (2000).
[18] R. Zwanzig, Acc. Chem. Res. **23**, 148 (1990).
[19] N. Agmon and J. J. Hopfield, J. Chem. Phys. **78**, 6947 (1983).
[20] H. Risken, *The Fokker-Planck Equation: Methods of Solution and Application* (Springer-Verlag, Berlin, 1984).
[21] A. Messiah, *Quantum Mechanics* (North-Holland, 1962).
[22] E. A. Evans, Annu. Rev. Biophys. Biomol. Struct. **30**, 105 (2001).
[23] J. Schlichter and J. Friedrich, J. Chem. Phys. **112**, 3045 (2000).